BUTTERWORTH HEINEMANN

Int. J. Fatigue Vol. 170, No. 3, pp. 221–227, 1995

0142-1123/95/$10.00

Fatigue crack growth behaviour of two contrasting titanium alloys

B.E. Powell

Department of Mechanical and Manufacturing Engineering, University of Portsmouth, Portsmouth PO1 3DJ, UK
(Received 13 September 1994; revised 25 October 1994)

Fatigue crack propagation rates have been measured for Ti–6Al–4V and Ti-5331S aeroengine disc materials using compact tension and corner-notched tensile testpieces. The loadings used simulate both the start–stop operations of aeroengines that lead to low-cycle fatigue and the in-flight vibrations that may cause high-cycle fatigue. It is suggested that the different fatigue crack growth behaviour of Ti-5331S, relative to that of Ti–6Al–4V, arises largely from the greater proportion of crack closure and short crack growth occurring in this alloy. Ti-5331S also exhibits a crack retardation effect due to the interaction between the processes of cyclic cleavage and striated crack growth which are associated with the high- and low-cycle fatigue components of the loading, whilst Ti–6Al–4V does not.

(Keywords: fatigue crack growth; corner notched specimen; combined high- and low-cycle fatigue; crack closure; crack retardation; Ti–6Al–4V; Ti-5331S)

The constant and insistent demand of those who own or operate gas turbine aeroengines is for increased performance combined with a lower cost of ownership. The aeroengine manufacturers have responded to this challenge, and for over 30 years part of their strategy has been to replace dense materials by titanium alloys, until they now constitute approximately a quarter of the weight of a large fan blade engine. This has been done despite the greater cost and lower stiffness of titanium alloys relative to steels, because the continuous development of low-density titanium alloys of high specific strength has given a substantial reduction in the weight of aeroengines, leading to greater thrust-to-weight ratios combined with lower fuel consumptions and greater payloads. Manufacturing versatility can also generate weight savings. The development of weldable high-strength titanium alloys permits the use of lighter welded rather than bolted assemblies, and an alloy having exceptional formability is essential for the fabrication of either hollow or honeycomb-cored wide chord fan blades. A versatile range of titanium alloys is now available, and they are widely used in aeroengine construction. Indeed it is now possible to specify titanium alloys for all the critical rotating components from the fan, operating at sub-zero temperatures, to the rear of the compressor stage, where the discharge temperature may reach 600 °C.

The current design limitation for aeroengine discs is that of low-cycle fatigue (LCF). In such rotating components the LCF loading arises from the cyclic variation of both the centrifugal and the thermal stresses. In the simplest case this major stress variation occurs once per flight. However, rotating engine components have also experienced high-cycle fatigue (HCF) failures as a direct result of excessive vibrational stresses. These minor stress cycles are characterized by a high frequency, and are superimposed on part of the major cycle. Consequently, in order that the fatigue integrity of these critical components might be fully assessed, it is necessary to establish the resistance of various disc and blade materials to the conjoint action of LCF and HCF loadings.

EXPERIMENTAL DETAILS

The two alloys selected for this study are the general-purpose $\alpha + \beta$ alloy Ti–6Al–4V and the near-α creep resistant alloy Ti-5331S. These alloys, which are also known as IMI318 and IMI829, show a marked contrast in terms of their microstructure, crack growth behaviour and temperature of application. Samples of both materials were cut from unused aeroengine discs. In the final stages of manufacture these discs were heat treated: the Ti–6Al–4V was solution treated at 960 °C, water quenched and aged at 700 °C, while the Ti-5331S was solution treated at 1050 °C, oil quenched and aged at 650 °C. As a consequence the Ti–6Al–4V consisted of regions of primary α and transformed β whose widths were approximately 25 μm (*Figure 1a*), while the Ti-5331S possessed a prior β grain size of 0.4 mm (*Figure 1b*). At room temperature the values of the 0.1% proof stress were 837 MPa and 760 MPa respectively.

Fatigue crack growth (FCG) rates have been determined using two specimen designs. A conventional compact tension (CT) testpiece generates data for long, through-the-thickness cracks; while a corner-notched (CN) testpiece (*Figure 2*), consisting of a square-sectioned bar containing a shallow notch at

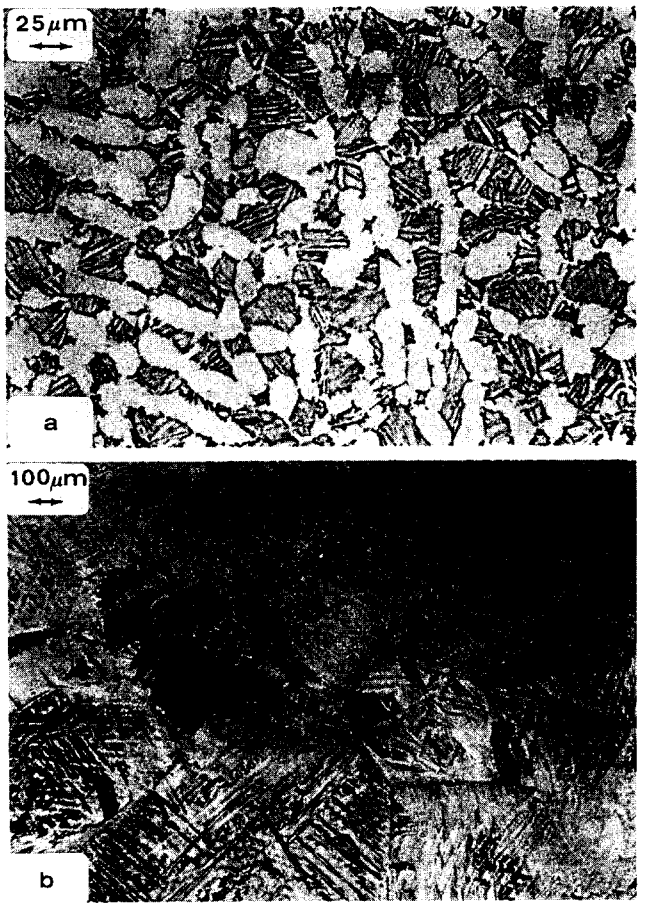

Figure 1 Microstructure of the test materials: (a) Ti–6Al–4V; (b) Ti-5331S

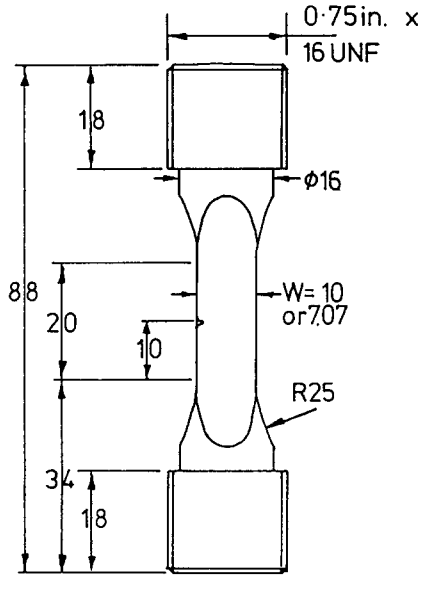

Figure 2 Corner-notched specimen (all dimensions in mm unless otherwise stated)

one corner, and loaded in remote tension, produces data for quarter circular cracks[1]. In terms of the nominal dimensions, the corner notches employed were 0.25 mm deep and 0.10 mm wide, and located in testpieces with cross-sectional areas of 50 or 100 mm^2 at their gauge lengths. The CT specimens were 26 mm wide and 13 mm thick and conformed to the British Standard[2] specified design.

A major cycle was represented in the fatigue testing by a trapezoidal stress wave, which was applied by a servohydraulic machine at a frequency of 0.1 Hz (*Figure 3a*). The rise and fall times were 1 s, while the dwell times at maximum and minimum load were 6.8 and 1.2 s. The minor cycles were simulated by a 150 Hz sinusoidal stress wave of constant amplitude generated by an electromagnetic vibrator, which was positioned between the servohydraulic actuator and the specimen. With this system the minor cycles may be superimposed upon that part of the major cycle corresponding to the cruise condition: that is, the dwell on maximum load, which was extended to accommodate the required number of minor cycles (*Figure 3b*). Allowing for the build-up and decay of the minor cycles at a frequency of 150 Hz, a 66.8 s dwell period gave an effective cycle of ratio 10000 minor cycles per major cycle.

The fatigue crack propagation characteristics of the two alloys were determined having first precracked the specimens to give an approximate crack length of 8 mm in a CT testpiece and 0.6 mm in a CN testpiece. During the subsequent collection of FCG data the levels of major and minor stress amplitude were maintained constant, so that as the test proceeded the levels of stress intensity range (ΔK) rose as the crack extended. Where possible, for tests involving the conjoint action of major and minor stress cycles, the approach adopted was to grow the crack from a low level of stress intensity range at which the minor cycles

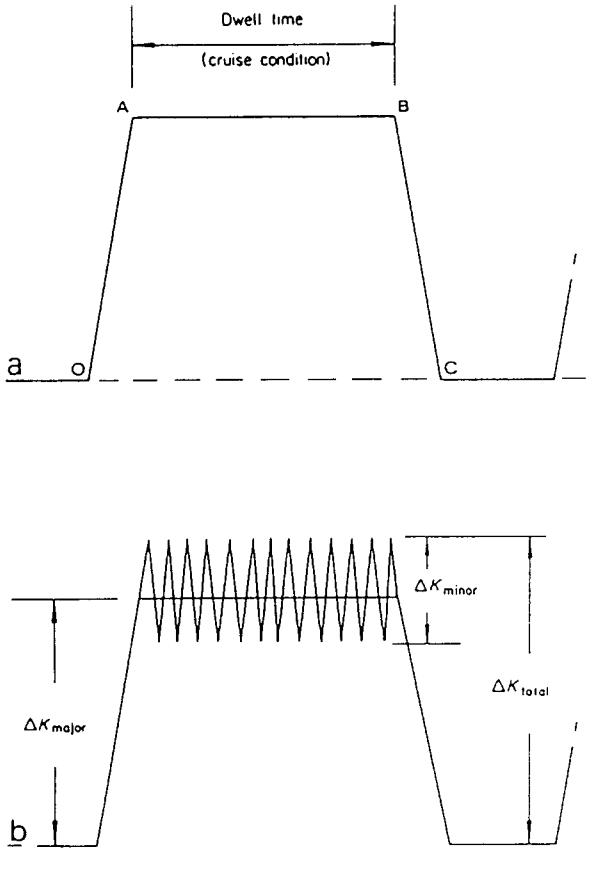

Figure 3 Fatigue loadings: (a) major cycle; (b) major and minor cycles

caused no growth, and by allowing the stress intensity range to rise unhindered, to determine both the FCG rates and the level of stress intensity range that marked the beginning of the contribution to the crack growth due to the presence of the minor cycles[3].

During every test, crack length was monitored using the direct current potential drop (DCPD) technique. The three-point secant method was used to determine crack growth rates, with input data corresponding to equal increments in the observed DCPD voltage ratio. In addition, bulk measurements of the crack opening load in the CT specimens have been made from plots of load versus back face strain recorded on an X–Y plotter both on loading and unloading. In order to accommodate the slow response of the plotter it was necessary to make a temporary reduction in the major cycle rise and fall times. Clearly the plotter could not follow the high-frequency minor cycles, and the load range recorded was that of the major cycle.

The fracture surfaces of the CT specimens were examined in a Jeol 35M scanning electron microscope equipped with vernier scales having a resolution of 0.002 mm. The photographs of each fracture surface were restricted to the centre line of each sample, and the distance from the centre of each field of view to the notch root was recorded in order that the associated value of ΔK might be determined.

RESULTS

The FCG rates in CT and CN specimens of Ti–6Al–4V subjected solely to major cycle loadings are in agreement for $\Delta K \leq 20$ MPa $m^{1/2}$. Above this level the rates diverge, and the slower rates of growth are associated with the CN specimen. This behaviour (*Figure 4*) is the same as that reported elsewhere for both Ti–6Al–4V and nickel-based superalloys[4,5]. However, the results obtained for the alloy Ti-5331S are in contrast to these findings, as the growth rates observed in the two types of specimen are essentially the same at all levels of ΔK examined (*Figure 5*).

Fatigue crack propagation experiments have been undertaken using 10000 minor cycles per major cycle (n), with a ratio of minor to major stress amplitudes (Q) of 0.12. These results (*Figures 6* and *7*) are presented as a function of ΔK_{total}, as this parameter accounts for the increase in stress intensity resulting from the superimposition of the minors on the major cycle. In Ti–6Al–4V both the CT and CN data show that the effect of the superimposed minor cycles is to give enhanced FCG rates, relative to the growth rates for major cycles alone (labelled $Q = 0$), above a transition level of ΔK_{total}. This transition has been labelled ΔK_{onset} as it corresponds to the onset of the minor cycle contribution to crack growth. It is apparent from *Figure 3b* that one half of one minor stress cycle has the effect of increasing the total or overall stress intensity range, and that:

$$\Delta K_{total} = \Delta K_{major} + \tfrac{1}{2}\Delta K_{minor} \quad (1)$$

The assumption that the crack growth increments associated with the overall cycle and the minor subcycles are independent then leads to the relationship

$$\frac{da}{dblock} = \left(\frac{da}{dN}\right)_{total} + [n - \tfrac{1}{2}]\left(\frac{da}{dN}\right)_{minor} \quad (2)$$

where da/dblock = the growth increment per loading block (*Figure 3a*); $(da/dN)_{total}$ = the growth increment associated with the application of the total, or peak-to-peak, stress intensity range; and $(da/dN)_{minor}$ = the growth increment associated with the application of the minor cycle stress intensity range. This linear

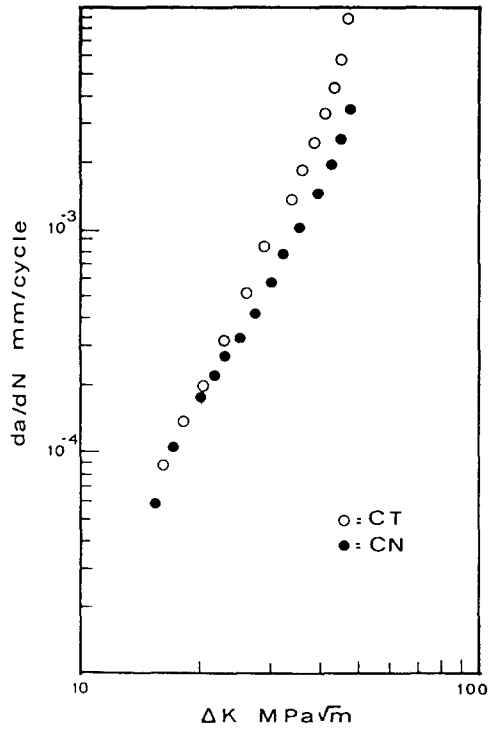

Figure 4 FCG rates generated in Ti–6Al–4V by a major cycle only loading

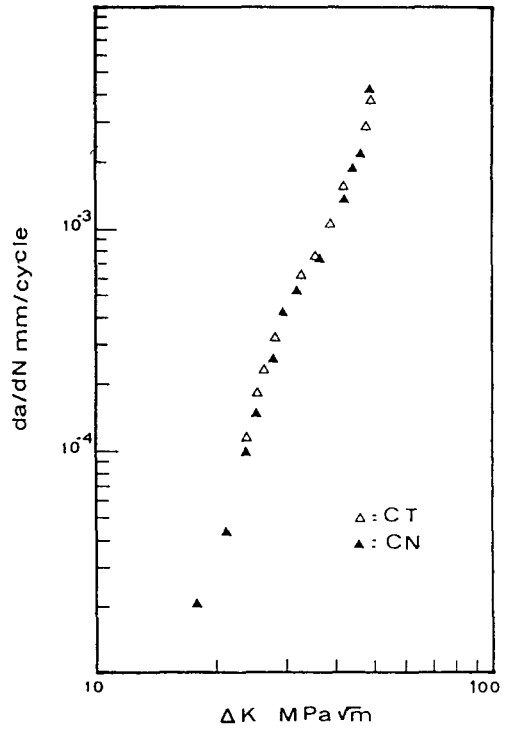

Figure 5 FCG rates generated in Ti-5331S by a major cycle only loading

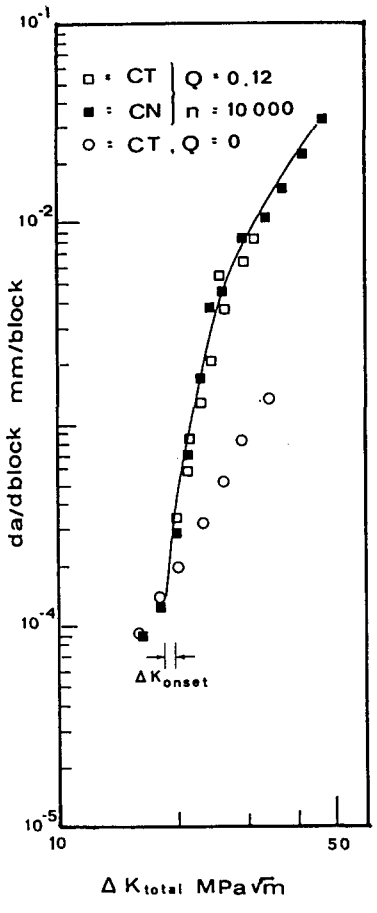

Figure 6 FCG rates generated in Ti–6Al–4V by combined major and minor cycles (Q = 0.12 and n = 10000) and by major cycles only (Q = 0)

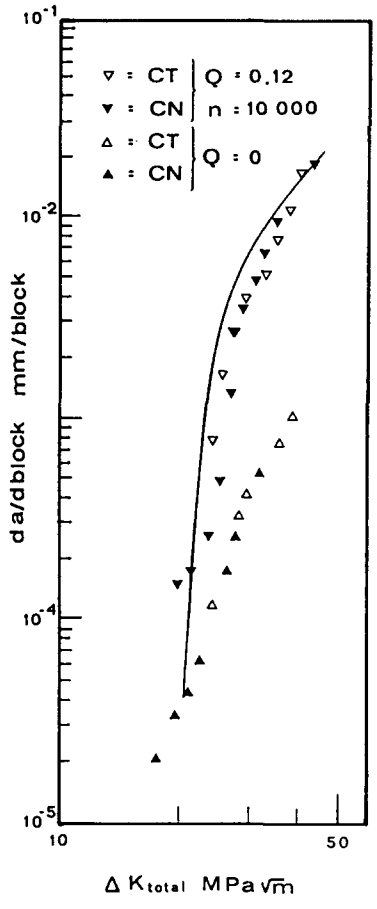

Figure 7 FCG rates generated in Ti-5331S by combined major and minor cycles (Q = 0.12 and n = 10000) and by major cycles only (Q = 0)

summation of the individual crack growth associated with the LCF and HCF loadings, indicated by a full line in *Figure 6*, gives an accurate prediction of the overall growth rates and the value of ΔK_{onset}. Thus, for this material, the linear summation predictions and the results from both the CT and the CN specimens are in accord.

In Ti-5331S, subjected to the previously stated combination of major and minor stress cycles, the measured growth rates show some departures from the linear summation predictions (*Figure 7*). Relative to these predictions, the long crack growth rates generated in CT testpieces show some retardation. In CN specimens the growth rates associated with the shorter crack lengths are greater than the linear summation predictions. Subsequently, as the length of the quarter-circular cracks increases, the growth rates again display some slight retardation. The initial enhancement in growth rates, which are associated with measurements at the shortest crack lengths, makes the determination of a ΔK_{onset} value difficult.

A comparison of *Figures 6* and *7* shows that the FCG rates in Ti-5331S are slower than those in Ti–6Al–4V when major cycles only are applied, but similar when the material is subjected to a combination of major and minor stress cycles.

Bulk measurements of crack closure have been determined for CT specimens using the back-faced strain method. In Ti-5331S the opening of the crack occurs at a level of stress intensity (K_{op}) that is virtually constant. In Ti–6Al–4V the levels of K_{op} are not only lower but also exhibit a rise that is linearly related to ΔK. This pattern of behaviour was observed both with major cycles applied separately and with combinations of major and minor stress cycles, the typical data presented (*Figures 8* and *9*) being for a combination of major and minor stress cycles.

The fracture surface of Ti-5331S can exhibit large cyclic cleavage facets because of the large grain size of the material; the surfaces are extensively covered by these facets within the near-threshold regime. For

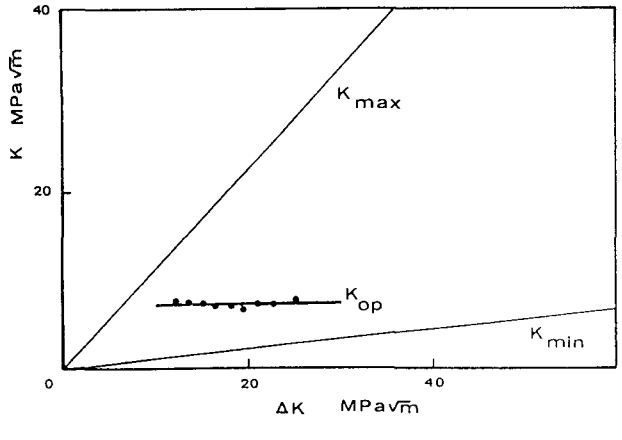

Figure 8 Typical crack closure behaviour in Ti-5331S

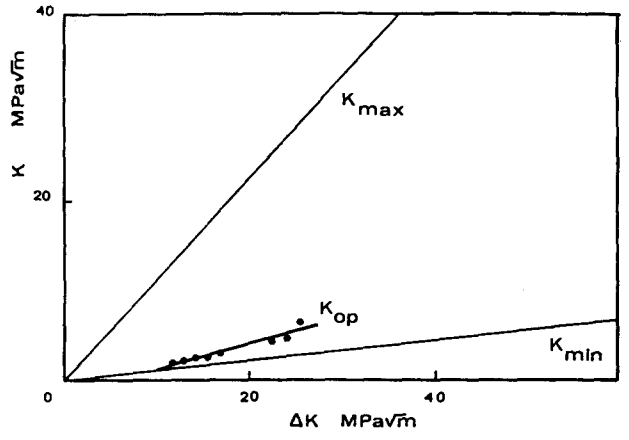

Figure 9 Typical crack closure behaviour in Ti–6Al–4V

major cycle only loadings, striation plateaux, some with secondary cracking, are readily detected when ΔK exceeds 27 MPa $m^{1/2}$; further increases in ΔK give greater striation spacings and the development of ductile tearing. In addition, the occurrence of crack closure within a major cycle may generate fretting-oxidation debris.

For a loading of combined major and minor stress cycles, the fracture surface topography prior to the onset of minor cycle crack growth is the same as that given by major cycle only loadings. Subsequently, the visible evidence of minor cycle contribution to growth is the development of 'block striations', which correspond to the periodic marking of the fracture surface by the major cycle loading, with the intervening crack advance resulting from the minor cycles of high stress ratio. The form of block striations in Ti-5331S, while on occasions similar to that in Ti–6Al–4V, generally differs in several respects[6]. First, at a cycle ratio of 10000, their occurrence is extensive (*Figure 10*) and they grow to a spacing of 30 μm. Second, rather than being replaced by cyclic cleavage facets they are frequently superimposed on them (*Figure 11*). Third, those block striations having an appearance of brittle striations exhibit a greater spacing than ductile striations in immediately adjacent areas (*Figure 12*). *Figure 13* shows an enlargement of the wide block striations seen in *Figure 12*, which have a brittle appearance. Here the block striations take the form of an irregular line of discrete pores from which many tear ridges develop.

DISCUSSION

The different crack closure mechanisms that occur in Ti-5331S and Ti–6Al–4V must give rise to the different K_{op} versus ΔK responses observed for these two materials. Thus the higher level of K_{op} observed in Ti-5331S is interpreted as resulting from the surface-roughness-induced crack closure, which derives from this material's larger grain size. The extent of this closure mechanism is largely controlled by the material's microstructure: thus the level of K_{op} remains virtually constant, at least in tests that largely span the intermediate region of FCG. By contrast, the lower level of K_{op} observed in Ti–6Al–4V is interpreted as resulting from the presence of plasticity-induced closure. The size of the plastic zone at the crack tip increases as ΔK increases, and as a consequence a progressive rise in K_{op} is to be expected, and is indeed observed.

The different FCG behaviour of the two titanium alloys, apparent when tested solely under a major cycle loading, can be rationalized on the basis of their crack closure characteristics in conjunction with the explanation for the growth rate discrepancy between specimen types advanced by Brown and Hicks[5]. They argue that the effect arises from a greater proportion of plane stress to plane strain in the CN specimen. In materials exhibiting a low level of crack closure due solely to crack tip plasticity, it may be expected that the extent to which a crack front is affected by crack closure will be influenced by the proportion of plane

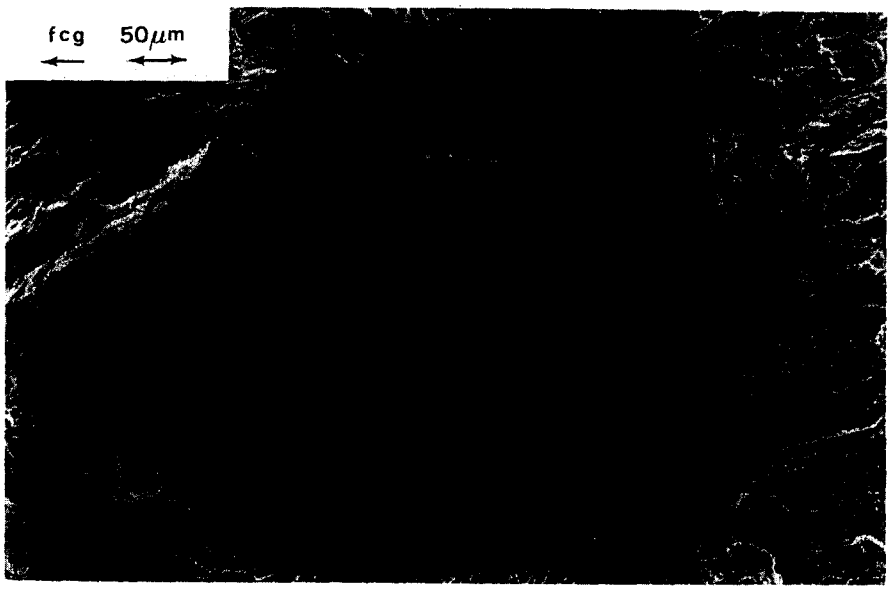

Figure 10 Division by tear ridges of a large block striation plateau (Q = 0.12, ΔK_{total} = 29.6 MPa $m^{1/2}$)

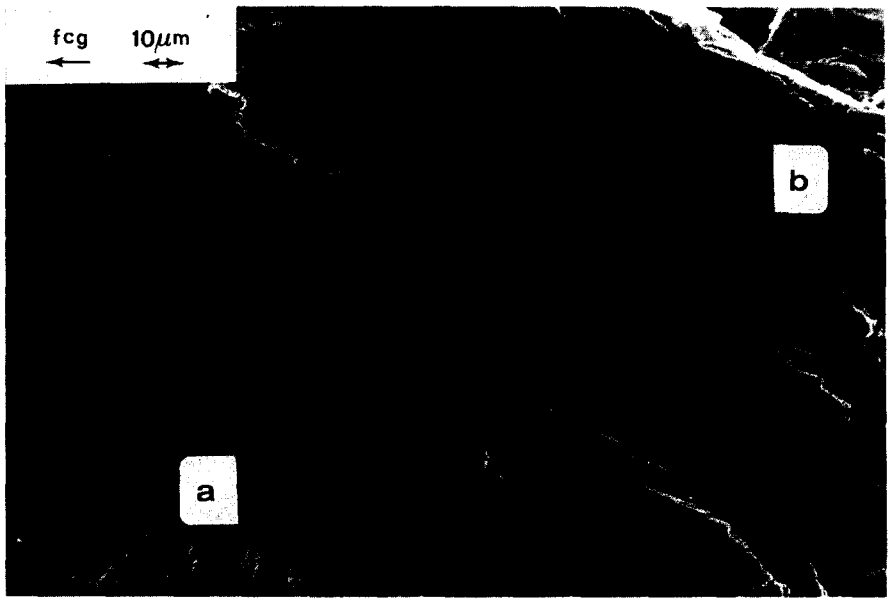

Figure 11 Block striations superimposed on: (a) cyclic cleavage facet; (b) fine transverse ripple markings (Q = 0.22, ΔK_{total} = 18.2 MPa $m^{1/2}$)

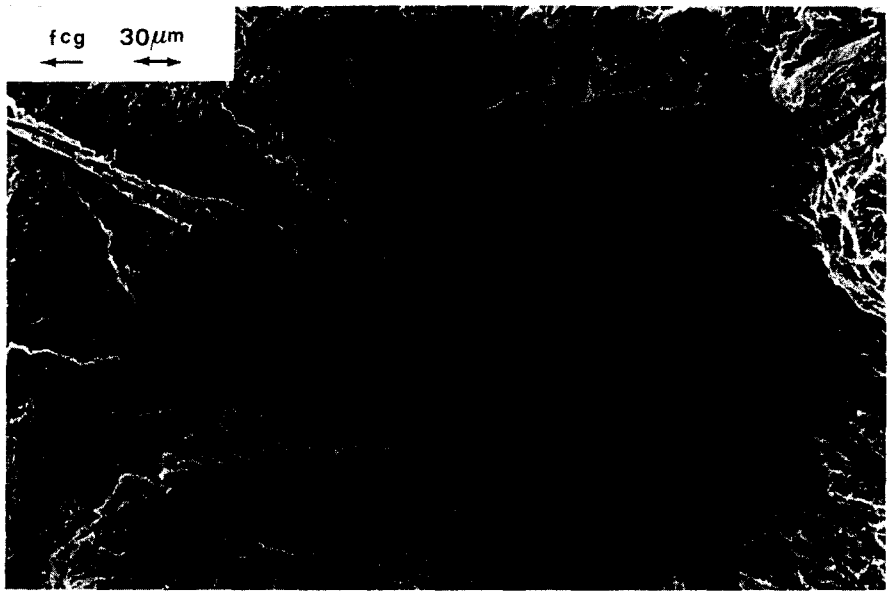

Figure 12 Large brittle striations continuous with finer ductile striations (Q = 0.12, ΔK_{total} = 37.1 MPa $m^{1/2}$)

stress to plane strain, and that a greater retardation in the rate of growth is to be expected if this proportion is increased. However, this effect will be insignificant for materials characterized by a high level of surface-roughness-induced crack closure that is microstructurally determined, as was observed for Ti-5331S.

In the absence of minor cycles Pickard *et al.*[4] have shown that the fatigue crack propagation lives associated with flaws in aeroengine discs are more accurately predicted using crack growth data from CN specimens. Where damaging minor cycles are present in substantial numbers their contribution to the overall growth rate is dominant. In these circumstances, differences between the FCG rates for major cycle loadings at $\Delta K \geqslant 20$ MPa $m^{1/2}$ become unimportant. This is the reason why the results from CN and CT specimens of Ti–6Al–4V subjected to combined low- and high-cycle fatigue, together with the linear summation predictions, can be in total agreement, although there is apparently a variation in one of the contributions to the overall crack growth.

The FCG rates predicted for Ti-5331S by the method of linear summation do not coincide entirely with those observed in either specimen design, thereby indicating the presence of additional forms of crack growth behaviour in this alloy. The growth rates that exceeded the linear summation predictions, observed in the CN specimens at the lowest levels of applied ΔK_{total}, corresponded to measurements taken when crack lengths were 1.5 to 4 times that of the grain size of the material: that is to say, at crack lengths for which the occurrence of microstructurally short crack effects might be expected. Brown and Hicks[7] have studied the extent of the microstructural short

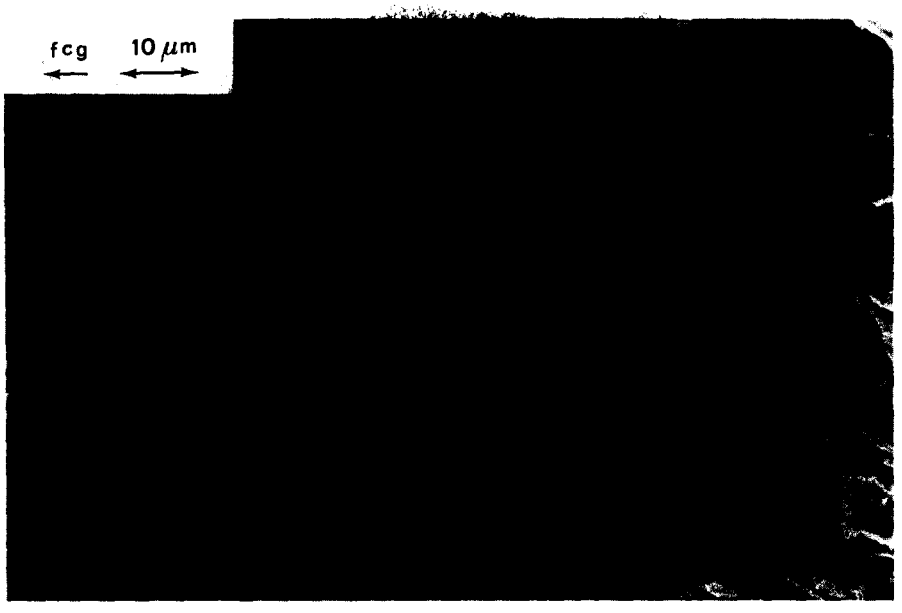

Figure 13 Development of tear ridges at block striations consisting of discrete and coalesced pores (Q = 0.12, ΔK_{total} = 36.5 MPa $m^{1/2}$)

crack effect for a variety of materials, including the influences of grain size and crystal structure, and have shown that the effect is substantial in a similar material, namely Ti-65S. Some additional tests have therefore been conducted using grain-coarsened Ti-5331S, and a similar enhancement in the FCG rates due to the behaviour of microstructurally short cracks has been observed.

Towards the end of the tests on Ti-5331S having grains of conventional size, when the crack length would be long and the values of ΔK_{total} are large, the results from both specimen designs indicate a retardation relative to the linear summation predictions. Forsyth[8] has suggested that any effective lengthening of the crack front will give a reduction in the crack growth rate. The periodic marking of the fracture surfaces with fatigue striations generated in response to the major cycle loading initiates many steps or tear ridges, perhaps as a consequence of either crack tip blunting or branching. Thus there is an increase in the total frontal length of the crack, which must now advance along a greater number of parallel cleavage planes, with the energy-absorbing process of ductile tearing occurring at the tear ridges. Under the influence of the intervening minor stress cycles the crack will grow by cyclic cleavage. As the crack propagates away from a striation the number and size of the tear ridges decline, but they are re-established at the next major cycle. Thus the interaction between the mechanisms of cyclic cleavage and striated crack growth can explain the incidence of retarded crack growth rates observed in Ti-5331S.

CONCLUSIONS

1. When the advance of a fatigue crack is used to generate a progressive increase in the stress intensity range applied to a compact tension testpiece, the bulk measurement of crack opening stress intensity in Ti-5331S remains almost constant, but rises linearly in Ti–6Al–4V.
2. Under a major cycle only loading the discrepancy in fatigue crack growth rates generated in compact tension and corner-notched testpieces above a stress intensity range of 20 MPa $m^{1/2}$, observed in Ti–6Al–4V, is absent in Ti-5331S.
3. In Ti–6Al–4V subjected to a combination of major and minor stress cycles there is agreement between the fatigue crack growth rates obtained from tests carried out on compact tension and corner-notched testpieces and those predicted by the linear summation of crack growth associated with the low- and high-cycle fatigue loadings.
4. In Ti-5331S both accelerations and retardations in growth rates relative to the linear summation predictions have been observed. These responses have been attributed to the behaviour of microstructurally short cracks and the interaction between the crack growth mechanisms of cyclic cleavage and striation formation when they occur alternately.

ACKNOWLEDGEMENT

The author wishes to thank Rolls-Royce, Aeroengine Division for the provision of funding, materials and technical support.

REFERENCES

1 Hicks, M.A. and Pickard, A.C. *Int. J. Fract.* 1982, **20**, 91
2 'British Standard Method for Determination of the Rate of Fatigue Crack Growth in Metallic Materials', BS 6835: 1988, British Standards Institution, Milton Keynes, UK, 1988
3 Powell, B.E. and Duggan, T.V. *Int. J. Fatigue* 1986, **4**, 187
4 Pickard, A.C., Brown, C.W. and Hicks, M.A. in 'Proc. Conf. Advances in Life Prediction Methods', New York, 1983, pp. 173–178.
5 Brown, C.W. and Hicks, M.A. *Int. J. Fatigue* 1982, **4**, 73
6 Powell, B.E. and Duggan, T.V. *Int. J. Fatigue* 1987, **9**, 195
7 Brown, C.W. and Hicks, M.A. Fatigue *Eng. Mater. and Struct.* 1983, **6**, 67.
8 Forsyth, P.J.E. 'A Unified Description of Micro and Macroscopic Fatigue Crack Behaviour', Technical Report 82065, Defence Research Agency, Farnborough, UK, 1982.